Available online at www.sciencedirect.com

ScienceDirect

Procedia Computer Science 108C (2017) 1582–1591

Procedia Computer Science

International Conference on Computational Science, ICCS 2017, 12-14 June 2017, Zurich, Switzerland

Feature Based Grid Event Classification from Synchrophasor Data

Sai Akhil R. Konakalla[1] and Raymond A. de Callafon[2]

[1] University of California San Diego, San Diego, U.S.A.
skonakal@ucsd.edu
[2] University of California San Diego, San Diego, U.S.A.
callafon@ucsd.edu

Abstract

This paper presents a method for automatic classification of power disturbance events in an electric grid by means of distributed parameter estimation and clustering techniques of synchrophasor data produced by phasor measurement units (PMUs). Disturbance events detected in the PMU data are subjected to a parameter estimation routine to extract features that include oscillation frequency, participation factor, damping factor and post and pre-event frequency offset. The parameters are used to classify events and classification rules are deduced on the basis of a training set of known events using nonlinear programming. Once the classification rules are set, the approach can be used to automatically classify events not seen in the training set. The proposed algorithm is illustrated on a Power Standards Lab microPMU system data for which frequency disturbance events were measured at UCSD over several months.

Keywords: synchrophasors, classification, grid events, clustering

1 Introduction

Recent growth in deployment of distributed energy resources (DERs), energy storage systems, and advanced grid control schemes have increased the levels of variability in generation and load conditions over the transmission and distribution system. Large scale decentralization of electricity production and rise in the adoption of micro-grids has made it even more difficult to monitor load or generation perturbations possibly caused by DER power production variability, load switching, (unintended) islanding, faults or line tripping. To overcome these challenges, many distribution systems operators (DSOs) have been focusing on developing methodologies that rely on robust information layers for the grid [1, 3, 4]. One of such layers include the use of the phasor measurement units (PMUs) for wide-area distributed networks [4] capable of measuring time-synchronized phasor (syncrophasor) data up to 60 Hz.

Widespread installation of PMUs has inspired the development of (real-time) synchrophasor applications [10, 13] for system monitoring, event (disturbance) detection and even automated

10.1016/j.procs.2017.05.046

grid control. The ability of these PMUs to time-synchronize three phase AC voltage and current phasor measurements from various points in a wide geographical distribution in a power grid with a precise global positioning system (GPS) clock has improved the feasibility of analyzing the operating status of a wide area power grid.

Although high sampling rate of PMUs is beneficial for grid protection, it also presents challenges in the storage and analysis of large volumes of data. To provide some solution to the storage and analysis problem, the event detection scheme in [9] provides an efficient solution of archiving data for analysis, only if a grid event or grid disturbance is detected. Hence, automated or semi-automated analysis techniques [5, 6, 12] to automatically classify grid events into relevant load or generation perturbations such as faults, out-of-step conditions, power generation anomalies are highly desirable. Such techniques greatly automate grid monitoring by extracting relevant information from PMU data and classify grid disturbance events.

Most of the power blackouts are typically caused by a single event that leads to cascading outages [14]. Clearly, it is critical to develop a PMU synchrophasor data analysis scheme that not only detects but also identifies the cause of these events to prevent potential cascading grid failures. This paper builds on a systematic data analysis procedure that uses the following 3 subsequent steps: event detection [3, 8, 9], parameter estimation [11, 18] and event classification [6, 12]. More specifically, the event detection involves detecting unusual occurrences of critical events in a power grid such as transient switching, outages, faults, line trips and intentional system test events like the Chief Joseph brake test. The parameter estimation involves estimating critical parameters of the disturbance event and extracting the features that relate these parameters to a specific type of event. Event classification involves grouping events according to its type, cause and extent of effect on the grid and attributing such events to specific components in the grid.

Data based event classification techniques such as neural networks, multiple linear regressions, generalized linear modeling, regression trees have been extensively studied [16]. Also, dimensionality reduction techniques such as principal component analysis (PCA) [2], [17] have become a great interest due to their faster computation features. However, the separate steps of event detection, parameter estimation and event classification have to be carried accurately and in a timely manner in order to prevent propagation of such outages or blackouts. The first step involving automated event detection has been recently addressed by in [9], whereas the next two steps are the focus of this paper. Additional event localization [3] can be used to identifying the approximate location of the origin of the event.

For the illustration and application of this methodology, real-time PMU data acquisition has been implemented for IEEE C37.118 formatted data from a microPMU system developed by Power Standards Lab (PSL). Event detection is performed in a distributed sense on a Raspberry PI processing the C37.118 data stream of a single PMU and detect events as described in [9]. It is shown how real-time processing of the phasor data received by C37.118 can be used to extract features which then can be used as a training set to classify recorded events. The training and testing data sets consist of event instances created from measurements of the single phase phasors (frequency) from the wall outlet in the Synchrophasor Grid Monitoring and Automation (SyGMA) lab at UCSD over several months.

2 Power Oscillations in Grid Dynamics

Modern power grids are mostly interconnected and operate close to the stability limits in transient and steady state modes [14]. Natural response of one group of closely coupled machines oscillate against one another in large interconnected grids. Higher frequency modes are localized with small groups that oscillate against each other. A small disturbance in any part of the system can initiate an inter-area oscillation, in a heavily interconnected grid. These oscillations, especially if lightly damped, can lead to a line trips due to protective relay trips and inducing a grid system collapse [15].

In a power system with multiple machines, measurements at nearby buses show coherent oscillation characteristics. As a result, changes in real power can be seen on frequency measurements while changes in reactive power can be seen in voltage measurements [14]. To illustrate the transient phenomenon in a largely interconnected power grid, consider a simple two-area power system model with two machines M1, M2 (each modeling generation and load) connected via a single bus.

Assuming that the machines M1 and M2 operating at voltages V_1 and V_2, start at initial angles δ_1 and δ_2 respectively with respect to reference nominal frequency and that M1 accelerates while M2 de-accelerates from their nominal rotation frequency. Excluding random variation of load caused by demands, let us consider only the frequency dependent load variation linearized with a coefficient β, allowing us to write

$$\frac{2H_1}{\omega_s}\ddot{\delta_1} = P_{m1} - P_{e1} + \beta_1\dot{\delta_1} \quad \text{and} \quad \frac{2H_2}{\omega_s}\ddot{\delta_2} = P_{m2} - P_{e2} + \beta_2\dot{\delta_2} \tag{1}$$

where P_{mi} indicates the mechanical power output in area i, P_{ei} indicates real power flow in/out of area i, H_i indicates the area inertia constant, ω_s indicates the synchronous frequency and subscripts $i = 1, 2$ refer to areas of M1 and M2 respectively. Assuming that the transmission line is lossless, with line impedance X, then power flows from M1 to M2 can be represented by

$$P_{e1} = -P_{e2} = \frac{V_1V_2}{X}\sin(\delta_{12}) \tag{2}$$

where $\delta_{12} = \delta_1 - \delta_2$. In steady state operation for the lossless transmission, the generated power at M1 is absorbed through M2 and therefore $P_{m1} = -P_{m2}$.

Combining the equations (1) and (2), one obtains

$$\begin{aligned} \tfrac{2H_1}{\omega_s}\ddot{\delta_1} - \tfrac{2H_2}{\omega_s}\ddot{\delta_2} &= 2P_{m1} + P_{e1} - P_{e2} + \beta_1\dot{\delta_1} - \beta_2\dot{\delta_2} \\ \tfrac{2H_1}{\omega_s}\ddot{\delta_1} - \tfrac{2H_2}{\omega_s}\ddot{\delta_2} &= 2P_{m1} - \tfrac{V_1V_2}{X}\sin(\delta_{12}) + \beta_1\dot{\delta_1} - \beta_2\dot{\delta_2} \end{aligned} \tag{3}$$

from which it can be seen that a two-area system with $H_1 = H_2 = H$, $\beta_1 = \beta_2 = \beta$, the normalized voltage units $V_1 = V_2 = 1$ and $P_{m1} = P_{m2} = 0$ follows

$$\ddot{\delta_{12}}(t) = -\omega^2\delta_{12}(t) - \beta_k\dot{\delta_{12}}(t) \tag{4}$$

under the assumption $\sin(\delta_{12}) \approx \delta_{12}$, valid for small values of the time t dependent $\delta_{12}(t)$. From (4) one recognizes a standard 2nd order differential equation that will have a sinusoidal solution with an (undamped) oscillation frequency $\omega = \sqrt{\frac{\omega_s}{HX}}$ rad/s and damping ratio $\beta_k = \frac{\omega_s\beta}{2H}$.

The purposes of the abovementioned analysis is to show that the power flow (2) of a two-area power system behaves much like a damped mass-spring system with natural (undamped) oscillation frequency $\omega > 0$ and damping ratio $0 \le \beta \le 1$. Since an electromechanical oscillation is an exchange of kinetic energy through electrical power between various machines, the oscillation takes a specific path through the grid [15]. In a large grid, e.g. the Western Electric Coordinating Council (WECC), there may be several such areas and the transmission system may have several resonance modes with coupling and possibly non-linear effects. The unavoidable phenomena of power oscillations due to rotating machine inertia will be exploited in the feature extraction whenever power disturbances occur on the grid.

3 Parameter Estimation for Feature Extraction

3.1 Free Response Dynamic Model

In a large interconnected grid (e.g. WECC) that can consist of several load-generation areas, it becomes very difficult to derive the swing equations due to highly coupled non-linear dynamic behavior between areas. As an alternative, we deploy system identification techniques to extract information from the grid each time an event occurs [11]. The realization algorithm [7] is used here to identify modal parameters of the power oscillation dynamics, assuming the free response of a linear dynamic behavior excited by a (im)pulse signal.

For the realization algorithm, consider a linear dynamic model

$$\begin{aligned} x(k+1) &= Ax(k) + Bu(k) \\ y(k) &= Cx(k) + Du(k) \end{aligned} \tag{5}$$

is used to capture the free response of the power oscillation or grid frequency oscillations $y(k)$ at discrete times, $t = k\Delta T, k = 0, 1, \ldots$ with a constant sampling time ΔT. In this paper we choose to use $y(k)$ to be the supply frequency $f(k)$ of the AC voltage signal as provided by a PMU. The motivation to use the measured AC supply frequency $f(k)$ is due to the strong correlation between $f(k)$ and real power flow $P(k)$ in a grid with rotating machinery as discussed in the the previous section. In addition, it is much easier to measure fluctuation in the AC supply frequency $f(k)$ via a PMU, without having to measure both AC voltage and AC current for power flow calculation. That said, feature extraction can also be applied to power measurements without loss of generality.

In (5), the vector $x(k) \in \mathbb{R}^{n\times 1}$ denotes a n-dimensional state vector, $A \in \mathbb{R}^{n\times n}$ is the state matrix, $B \in \mathbb{R}^{n\times 1}$ is the input matrix, $C \in \mathbb{R}^{1\times n}$ is the output matrix and $D \in \mathbb{R}^{1\times 1}$ is the feedthrough scalar/matrix with C and D having (only) a single row, the analysis presented here assumes a single (output) measurement. However, the approach can be easily extended to multiply synchronized PMU measurements where C and D have may multiple rows. With the model (5), the (impulse) input $u(k)$ and power or frequency measurement $y(k)$ are related via the Markov parameters $g(k) = CA^{k-1}B$ for $k > 0$ and allow the input/output dynamic relation to be written as a discrete-time convolution

$$y(k) = Du(k) + \sum_{j=1}^{\infty} g(j)u(k-j)$$

where $y(k) = g(k)$ due to the (im)pulse input $u(k)$. Our goal is to estimate the order n of the model and then compute (realize) the matrices A, B and C of the model based on discrete-time power or frequency swing observations $y(k)$. These matrices are then used to extract the relevant parameters to quantify the event.

3.2 Realization Algorithm for Model Estimation

For the realization algorithm, one uses $2N$ discrete-time measurements $y(k),\ k = 1, 2, \ldots, 2N$ to construct a Hankel matrix H and the corresponding shifted Hankel matrix $\bar{H}$ of the same size given by

$$H = \begin{bmatrix} y(1) & y(2) & \cdots & y(N) \\ y(2) & y(3) & \cdots & y(N+1) \\ \vdots & \vdots & \ddots & \vdots \\ y(N) & y(N+1) & \cdots & y(2N-1) \end{bmatrix} \quad \text{and} \quad \bar{H} = \begin{bmatrix} y(2) & y(3) & \cdots & y(N+1) \\ y(3) & y(4) & \cdots & y(N+2) \\ \vdots & \vdots & \ddots & \vdots \\ y(N+1) & y(N+2) & \cdots & y(2N) \end{bmatrix}$$

where it can be shown that $\bar{H} = H_1 A H_2$ where $H_1 \in \mathbb{R}^{N \times n}$, $H_2 \in \mathbb{R}^{n \times N}$ are a rank n decomposition $H = H_1 H_2$ of the Hankel matrix H. Such a rank n decomposition can be computed via a Single Value Decomposition (SVD) $H = U \Sigma V^T$ where $U, V \in \mathbb{R}^{N \times N}$ are orthonormal matrices and $\Sigma \in \mathbb{R}^{N \times N}$ is a diagonal matrix with N singular values ordered in a non-decreasing magnitude on the main diagonal.

Choosing a fixed model order n, the SVD allows a rank n approximation $H \approx U_n \Sigma_n V_n^T$ of the full rank N matrix H, where $U_n \in \mathbb{R}^{N \times n}$ indicates the first n columns in U, $\Sigma_n \in \mathbb{R}^{n \times n}$ the first n rows and n columns of Σ and $V_n \in \mathbb{R}^{N \times n}$ indicates the first n columns in V. The rank n approximation rewrites $H \approx H_1 H_2$ where $H_1 = U_n \Sigma_n^{1/2}, H_2 = \Sigma_n^{1/2} V_n^T$ and the state space matrices A, B, C can be computed using $A = \Sigma_n^{-1/2} U_n^T \bar{H} V_n \Sigma_n^{-1/2}$, $B = H_2(:,1)$ and $C = H_1(1,:)$, where $H_2(:,1) \in \mathbb{R}^{n \times 1}$ denotes the first column in H_1 and $H_1(1,:) \in \mathbb{R}^{1 \times n}$ denotes the first row of H_1.

3.3 Model Based Feature Extraction

For feature extraction we consider transient dynamic behavior stability of the model, determined by the eigenvalues λ_i, $i = 1, 2, \ldots, n$ of the estimated state matrix A. In addition to the eigenvalues of A, also the nullspace solutions to $[A - \lambda_i I]\phi_i = 0$ and $\psi_i[A - \lambda_i I] = 0$ are computed to find the left ψ_i and right ϕ_i eigenvectors. The information on the (complex) eigenvalues λ_i, left ψ_i and right ϕ_i eigenvectors are now used to compute the main dynamic features of a power of frequency oscillation event $y(k)$, $k = 1, 2, \ldots$: the oscillation frequencies f_i, damping ratios ζ_i and relative participation factors P_i of the event, respectively given by

$$f_i = \frac{|s_i|}{2\pi}, \zeta_i = \frac{-a_i}{2\pi f_i}, P_i = |\phi_i \psi_i| \tag{6}$$

where $s_i = 60 \ln(\lambda_i) = a_i \pm j b_i$ for 60Hz sampling of the data $y(k)$.

The frequency f_i, damping ζ_i and participation factor P_i, collectively called the (dynamic event) parameters in (6) are used to characterize the dynamic aspects of an observed event and motivated as follows. Firstly, oscillating areas may be characterized by different modes or oscillation frequencies f_i. Secondly, the damping factor ζ_i plays an important role in determining the nature of the oscillation mode and will help in deciding whether the disturbance event occurred in the main or local grid area. For example, it was found that undamped oscillations at about 0.33 Hz was the major restraint on a larger transfer [15] in the WECC system caused by generator high gain automatic voltage regulators (AVR). Next, the participation factors P_i can be used to characterize the relative contribution of each oscillation mode and decide the source of the oscillation event. Finally, next to the listed (dynamic event) parameters in (6) that capture the dynamic behavior of a power oscillation event, also the static behavior is used in event characterization. The static parameter is characterized by the post-event deviation of the measured frequency amplitude ΔF before and after the event and computed via

$$\Delta F = \frac{1}{N_1} \sum_{k=N_1-k_0}^{k_0-1} y(k) - \frac{1}{N_2} \sum_{k=k_0+N}^{k_0+N+N_2-1} y(k)$$

where N_1 is the number of data points before the event at time index $k = k_0$ and N_2 is the number of data points after the event has settled at time index $k = k_0 + N$.

4 Feature Based Clustering for Grid Event Classification

Computational techniques such as distribution based cluster analysis, a type of unsupervised machine learning can be used to identify different patterns. In this paper, the k-nearest neighbor algorithm is used to find patterns and classify the event. The k-means clustering method is a method used in a p-dimensional space, with an L_1-norm distance measure used for minimization of the distance from the point to centroid. The L_1 is the sum of absolute differences, also known as the 'city block distance'.

The goal of the algorithm is to partition the given data $\{x_1, x_2, ..., x_n\} \in \mathbb{R}^d$ into k disjoint clusters $\mathcal{C} = \{C_1, ..., C_k\}$ such that the sum of the cluster elements from the cluster centroid is minimized. Each centroid is the component-wise median of the points in that particular cluster. Formally, the problem can be formulated. Given a set of k cluster centers $C = \{c_1, ..., c_k\}$, where $x, c \in \mathbb{R}^d$, the k-means objective function for L_1 distance minimization is given by

$$J(\mathcal{C}, C) = \sum_{j=1}^{k} \sum_{x_i \in C_j} |x_i - c_j| \tag{7}$$

and the cost function $J(\mathcal{C}, C)$ (7) is non-convex. As a result, the problem of finding the global minimum of the k-means objective needs to be solved via a non-linear minimization, initialized at an initial centroid value c_j.

Once clustering has been achieved, it is worthwhile to give the computed clusters C a meaningful interpretation. The interpretation can be based on the fact that power system oscillations are classified by the system components that they effect. Traditionally, oscillation modes are classified based on oscillating frequencies alone [19], although damping is included in most calculation. The classical frequency distinction results in so-called interarea mode oscillations ($f <\leq 1$ Hz and typically around 0.3 Hz), local plant mode oscillations ($1.0 < f \leq 2.0$ Hz), intraplant mode oscillations ($2.0 < f <\leq 3.0$ Hz), torsional mode oscillations ($10 < f < 16$ Hz) and control mode oscillations. But the participation P_i of each such oscillating frequencies is often overlooked. In some cases, there might be an event caused by more than one of such modes of oscillation. Hence consideration of participation factor of each of such participating mode would provide better insights for classification.

5 Application of Clustering PMU Frequency Data

5.1 Frequency and Participation Factor Clustering

To illustrate the clustering of oscillation modes based on frequency domain data, PMU data acquisition has been implemented for IEEE C37.118 data from the microPMU system developed by Power Standards Lab (PSL). Event detection is performed as described in [9] and detect events based on the single phase AC supply frequency measurements from the wall outlet in the lab over several months. Using the set of measured events, first the k-means clustering algorithm is applied to a 2-dimensional space with natural frequency f_i of oscillation and the participation factor P_i of that oscillation frequency f_i. The resulting number of clusters are chosen to be 4 and the results of the feature (frequency f_i and partition factor P_i) extraction is depicted in Fig. 1. From the automated clustering results depicted in in Fig. 1, the following interesting conclusions may be drawn. Cluster 1 may be defined as the cluster containing the very-low frequency interarea (VLFI) oscillations of the grid. These oscillations occur in almost every detected event usually at a higher participation factors $P_i > 40\%$. These oscillations are

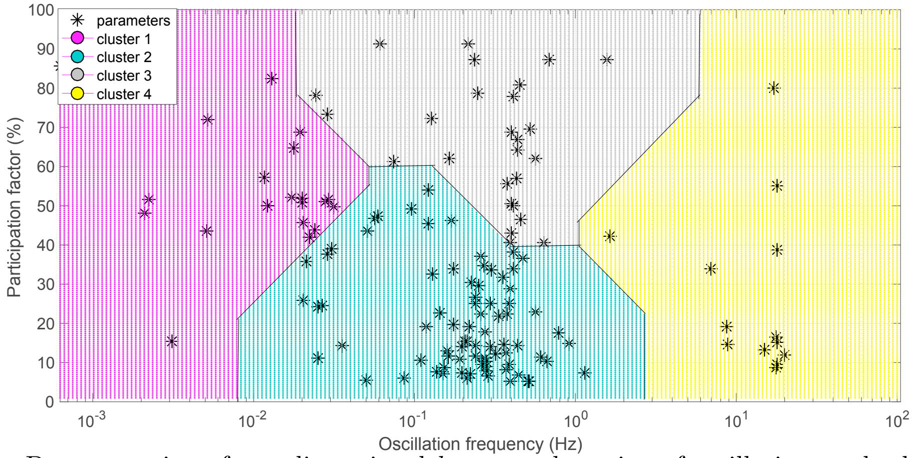

Figure 1: Demonstration of two-dimensional k-means clustering of oscillation modes based on oscillation frequency f_i and participation factor P_i.

a result of large coherent generation areas in the WECC system swinging against each other and hence can be seen for almost every excitation in the WECC system. These oscillations do not provide any useful information in event classification as they inadvertently occur in almost every event. Cluster 2 may be defined as the cluster containing the low participation frequency interarea (LPFI) oscillations of the grid. These consist of the typical interarea oscillations in the WECC system that exhibit frequency oscillations of $f_i \sim 0.3$ and have a lower participation P_i in the events. Moreover, this is usually associated with a frequency component from Cluster 1. Cluster 3 may be defined as the cluster containing the high participation frequency interarea (HPFI) oscillations of the grid. These consist of the typical interarea oscillations in the WECC system that exhibit frequency oscillations of $f_i \sim 0.3$ Hz and have a significant participation P_i in any grid event. Finally, Cluster 4 may be defined as the cluster containing the frequency torsional mode (FT) oscillations of the grid. Usually these modes are excited when a multi-stage turbine generator is connected to the grid system through a series compensated line.

5.2 Frequency, Participation Factor and Damping Clustering

Although the above description may provide an intuitive clustering of events, the clustering approach in this paper can be extended to allow further classification based on damping ratio. This method of classification helps differentiate between oscillations initiated in the local or the main grid in the WECC system due to variation of damping levels in each of these cases. Hence, three-dimensional k-means clustering involving natural frequency of oscillation f_i, participation factor P_i and damping factor ζ_i is performed. We keep the same number of 4 clusters as in Fig 1, but include damping ratio as the third dimension for classification. The clustering results are shown in Fig. 2. The 3-dimensional clustering provides an intuition about the events that occur locally (close to the measurement point) or non-locally (far-off from the measurement point). Cluster 1 contains very low frequency components with very high damping which does not contain any signature of an event. Hence components falling in cluster 1 can be ignored for classification of events into local/non-local events. Cluster 2 may be defined as the cluster containing frequency components around 0.3 Hz WECC frequency with low participation, low damping factor signifying that these may be the components present in the local grid events. Cluster 3 may be defined as the cluster containing frequency components

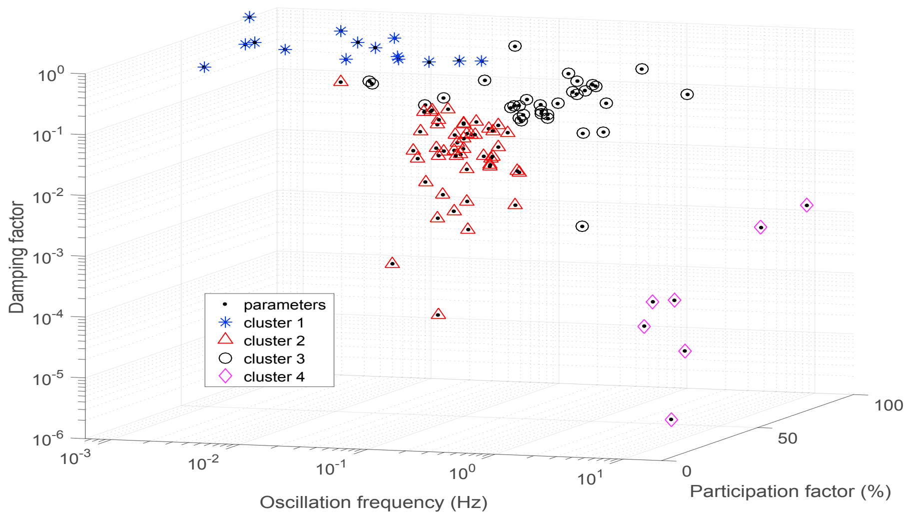

Figure 2: Demonstration of three-dimensional k-means clustering of oscillation modes based on oscillation frequency f_i, participation factor P_i and damping factor ζ_i for classification of oscillation modes at different damping levels.

around 0.3 Hz WECC frequency with high participation, high damping factor signifying that these may be the components present in the non-local events such as the Chief Joseph break test. Cluster 4 depicts high frequency torsional oscillations that occur at very low levels of damping signifying local events.

5.3 Steady State Frequency Deviation Clustering

Finally, single dimensional classification of grid events resulting in steady state frequency deviations can also be performed. Application of the k-means clustering on the difference of the frequency before and after the event ΔF in (3.3) will provide additional information on a particular grid event in terms of steady state power loss or power surplus. These events may be caused due to unexpected generation trip or sudden load loss in an area. The resulting clusters based on ΔF are shown in Fig. 3. The events that fall in Cluster 1 do not show any significant steady state frequency level ΔF deviation and hence do not fall under generation loss events. Whereas the events in Cluster 2 show a steady state frequency deviation $\Delta F > 0.04$ Hz and can be interpreted as generation surplus (or load loss) during the event.

5.4 Validation on PMU Data Events

The deduced rules for event classification of grid event can be applied on a set of events not used for (the training of) the clustering algorithm. This validation will demonstrate the robustness of the classification algorithm. For this purpose frequency PMU data from three measured known events are used: (1) the Chief Joseph Brake test on April 14^{th} 2015 (WECC event), (2) the disturbance caused during a major Tornado warning issued in San Diego on January 6^{th} 2016 (local event) and (3) the loss of major resources in Montana (generation loss) on January 21^{st} 2016 measured from Coronado substation. Table 1 shows the classification of these three events based on the clustering computed on the training set of events. The cluster components

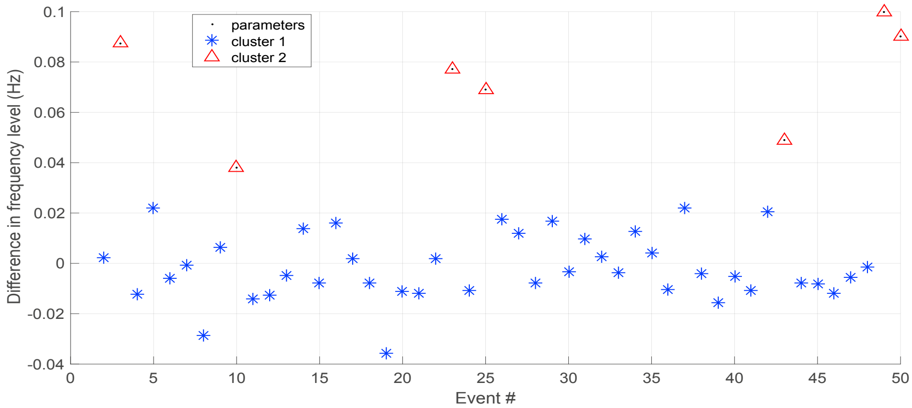

Figure 3: Demonstration of single dimensional k-means clustering of events based on difference of frequency amplitude ΔF before and after the event as in (3.3) for classification of events.

of the first event fall in cluster 1 (VLFI) and cluster 3 (HPFI) of the first classifier, cluster 3 (non-local) of the second classifier and cluster 1 of the third classifier. Hence, this event can be classified as a HPFI, non-local event without any power loss. Similarly, the cluster components of the second event fall in cluster 1 (VLFI) and cluster 2 (LPFI) of the first classifier, cluster 2 (local) of the second classifier and cluster 1 of the third classifier. Hence, this event can be classified as a LPFI, local event without any power loss. Finally, the cluster components of the third event fall in cluster 1 (VLFI) and cluster 3 (HPFI) of the first classifier, cluster 3 (non-local) of the second classifier and cluster 2 of the third classifier. This event can be classified as a HPFI, non-local event with generation loss, affirming the credibility of the algorithm.

Test Events (Cluster)	**Classifier 1**				**Classifier 2**				**Classifier 3**	
	$\mathcal{C}1$	$\mathcal{C}2$	$\mathcal{C}3$	$\mathcal{C}4$	$\mathcal{C}1$	$\mathcal{C}2$	$\mathcal{C}3$	$\mathcal{C}4$	$\mathcal{C}1$	$\mathcal{C}2$
Event 1 (April 14^{th}, 2015)	X	-	X	-	X	-	X	-	X	-
Event 2 (January 6^{th}, 2016)	X	X	-	-	X	X	-	-	X	-
Event 3 (January 21^{st}, 2016)	X	-	X	-	X	-	X	-	-	X

Table 1: Assessment of classification algorithm based on test events

6 Conclusions and Future work

This paper shows combining estimation of dynamic event parameters combined with standard clustering methods can be used to build classifiers to quantify power grid oscillation events on synchrophasor data. The event parameters included frequencies, damping and participation factors of each oscillation mode in an event and can be estimated by realization algorithm. Application of the feature based grid event classification to actual PMU synchrophasor data obtained from a microPMU shows realistic clustering based classification of various detected disturbance events. Our future work will implement the event classification algorithm in real-time on a PMU connected client computer to detect and automatically classify grid events.

References

[1] A. Allen, M. Singh, and E. Muljadi. PMU data event detection: A user guide for power engineers. Technical report, NREL/TP-5D00-61664, 2014.

[2] Olivier Antoine and Jean-Claude Maun. Inter-area oscillations: Identifying causes of poor damping using phasor measurement units. In *2012 IEEE Power and Energy Society General Meeting*, pages 1–6. IEEE, 2012.

[3] Omid Ardakanian, Ye Yuan, Roel Dobbe, Alexandra von Meier, Steven Low, and Claire Tomlin. Event detection and localization in distribution grids with phasor measurement units. *arXiv preprint arXiv:1611.04653*, 2016.

[4] Milan Biswal, Sukumar Brahma, and Huiping Cao. Supervisory protection and automated event diagnosis using pmu data.

[5] Rajkumar Buyya, Rodrigo N Calheiros, and Amir Vahid Dastjerdi. *Big Data: Principles and Paradigms*. Morgan Kaufmann, 2016.

[6] Yang Chen, Le Xie, and Panganamala Ramana Kumar. Power system event classification via dimensionality reduction of synchrophasor data. In *2014 IEEE 8th Sensor Array and Multichannel Signal Processing Workshop (SAM)*, pages 57–60. IEEE, 2014.

[7] Raymond A De Callafon, Babak Moaveni, Joel P Conte, Xianfei He, and Eric Udd. General realization algorithm for modal identification of linear dynamic systems. *Journal of engineering mechanics*, 134(9):712–722, 2008.

[8] Do-In Kim, Tae Yoon Chun, Sung-Hwa Yoon, Gyul Lee, and Yong-June Shin. Wavelet-based event detection method using pmu data.

[9] Sai Konakalla and Raymond de Callafon. Optimal filtering for grid event detection from real-time synchrophasor data. *Procedia Computer Science*, 80:931–940, 2016.

[10] J. Liu, G.and Quintero and V. Venkatasubramanian. Oscillation monitoring system based on wide area synchrophasors in power systems. In *Proc. iREP Symposium on Bulk Power System Dynamics and Control*, pages 1 – 13, 2007.

[11] L. Ljung. *System Identification - theory for the user*. Prentice Hall, Upper Saddle River, NJ, 1999.

[12] Duc Nguyen, Richard Barella, Scott A Wallace, Xinghui Zhao, and Xiaodong Liang. Smart grid line event classification using supervised learning over pmu data streams. In *Green Computing Conference and Sustainable Computing Conference (IGSC), 2015 Sixth International*, pages 1–8. IEEE, 2015.

[13] J.B. Roberts and D. Tziouvaras. Fault type selection system for identifying faults in an electric power system. *U.S. Patent 6,525,543*, 2003.

[14] Hadi Saadat. *Power system analysis*. WCB/McGraw-Hill, 1999.

[15] FR Schleif and JH White. Damping for the northwest-southwest tieline oscillations-an analog study. *IEEE Transactions on Power Apparatus and Systems*, (12):1239–1247, 1966.

[16] Glenn W Stagg and Ahmed H El-Abiad. *Computer methods in power system analysis*. McGraw-Hill, 1968.

[17] F.A. Tobar, L. Yacher, R. Paredes, and M.E. Orchard. Anomaly detection in power generation plants using similarity-based modeling and multivariate analysis. In *Proc. American Control Conference*, pages 1940–1945, San Francisco, CA, USA, 2011.

[18] P. Tripath, S.C. Srivastava, and S.N. Singh. An improved prony method for identifying low frequency oscillations using synchro-phasor measurements. In *Proc. International Conference on Power Systems*, pages 1–5, 2009.

[19] Y. Yuan, Y. Sun, L. Cheng, G. Chen, and P. Wang. Power system low frequency oscillation monitoring and analysis based on multi-signal online identification. *Science China Technological Sciences*, 53:2589–2596, 2010.